IEEE Access
Multidisciplinary | Rapid Review | Open Access Journal

Date of publication xxxx 00, 0000, date of current version xxxx 00, 0000.

Digital Object Identifier 10.1109/ACCESS.2017.Doi Number

Characterization of PDIV, PDEV and RPDIV in Insulated Wires under Unipolar Repetitive Square Wave Excitations for Inverter-Fed Motors

Hadi Naderiallaf[1], Paolo Giangrande[2], and Michael Galea[3]

[1]Power Electronics, Machine and Control Group (PEMC), University of Nottingham, Nottingham NG7 2RD, U.K.
[2]Department of Engineering and Applied Sciences, University of Bergamo, Bergamo, 24129, Italy
[3]Department of Industrial Electrical Power Conversion, University of Malta, 2080 Msida, Malta

Corresponding author: Hadi Naderiallaf (Hadi.Naderiallaf@nottingham.ac.uk).

This work was supported by the Clean Sky 2 Joint Undertaking through the European Union's Horizon 2020 Research and Innovation Programme under Grant 807081.

ABSTRACT The behaviour of partial discharge inception voltage (PDIV), partial discharge extinction voltage (PDEV) and repetitive partial discharge inception voltage (RPDIV) as a function of exposure/poling time under unipolar repetitive square wave excitations at atmospheric pressure (1013 mbar) is experimentally measured and investigated. The partial discharge (PD) tests are performed on two commercially available insulated wires: Glass fibre as Type II and Polyether Ether Ketone (PEEK) as Type I insulated wires used in inverter-fed motors. The impact of excitation polarity, pulse repetition frequency and rise time on the PD quantities (i.e., PDIV, PDEV and RPDIV) is studied as a function of stressing duration. In addition, the trend of RPDIV and PDIV dispersion levels are compared as a function of poling time under positive and negative unipolar excitations with two rise times (i.e., 80 and 800 ns) and two pulse repetition frequencies (i.e., 50 Hz and 2.5 kHz), relying on the shape/slope parameter of the Weibull distribution. The collected data shows that the electric field induced by the interface charge deposited by PD occurring during consecutive pulses and the space charge accumulation in the insulation bulk plays a decisive role in PD quantities' variations under unipolar repetitive square wave excitations.

INDEX TERMS Electric machines, partial discharges, pulse width modulation, space charge, variable speed drives.

I. INTRODUCTION

High *dV/dt* power converters improve both power density and loss reduction by delivering faster rise times, higher switching frequencies, increased DC link voltages, and easier thermal management [1], [2], [3], [4], [5], [6]. The higher *dV/dt* of inverter impulses, the higher voltage falls in the first turn of the machine winding due to impedance mismatch [7], enhancing the risk of partial discharge (PD) between the turn-to-turn insulation. The winding insulation may prematurely fail due to ongoing PD activity, especially for organic insulating materials, compromising the electrical machine operations [8], [9]. Hence, the reliability of the electric drive chain is dominated by the probability of turn-to-turn insulation failure [10]. The PD-free criterion, which states that the minimum partial discharge inception voltage (PDIV) must be greater than the peak voltage between two adjacent turns, should therefore be followed when designing low-voltage electrical machines [9].

For low-voltage (Type-I insulation, < 700 V_{rms}) and high-voltage (Type-II insulation, > 700 V_{rms}) rotating machines, the International Electrotechnical Commission (IEC) established two technical standards, namely IEC 60034-18-41 and IEC 60034-18-42 [11], [12]. These standards note that PDIV and endurance tests should be carried out on the two types of rotating machines [13]. PD inception is the end-of-life criterion for Type I insulations (i.e., organic insulating materials, e.g., polyamide-imide), requiring a PD-free insulation design [9]. Therefore, using Type II insulations (i.e.,

mixed organic-inorganic insulating materials, so-called corona-resistant materials), which ostensibly can sustain PD activity, is another solution frequently suggested by manufacturers, introducing a paradigm shift. Type II insulations are characterized by improved endurance at ground level (i.e., automotive applications), even though they are not a practical alternative at decreased pressures (i.e., aerospace applications). It is due to the promoted energetic content of discharges at reduced pressures, which increases their destructive potential, giving an instant failure if operated above PDIV [14].

In this study, Glass fibre and Polyether Ether Ketone (PEEK) insulated wires are considered (i.e., Type II and Type I insulation respectively) and tested at atmospheric pressure (1013 mbar) and room temperature. This comparative study aims to show that the PD quantities (i.e., PDIV, PDEV and RPDIV) can change as a function of exposure time to unipolar excitations for the two different insulated wires.

IEC 60034-18-41 and IEC 60034-18-42 (i.e., [11] and [12]) are the available standards corresponding to design qualification, type, and quality control tests of insulation systems used in inverter-fed motors. They express that PD measurements can be performed under sinusoidal waveforms or repetitive voltage impulse excitations for testing system components. However, the electric field distribution and PD behaviour are different under the sinusoidal waveform and bipolar impulse voltages compared with unipolar excitations even at the same peak-to-peak voltage. For example, the measured peak-to-peak values of PDIV under unipolar impulse voltages are lower than the obtained peak-to-peak PDIV values under bipolar voltages at the same rise time and switching frequency under atmospheric pressure (1013 mbar) [15]. The space charge accumulation in the insulation bulk and interface charge deposited by PD can modify the electric field intensity in the air gap between the two wires (i.e., adjacent turns), increasing or mitigating PDIV. An electric field reduction can occur in the air gap owing to heterocharge space charge accumulation (i.e., the space charge polarity is opposite to that of the neighbouring electrode). The opposite holds for the homocharge space charge accumulation (i.e., the space charge polarity is the same as that of the adjacent electrode) [16]. Due to the presence of a DC component, the accumulation of space charges in the insulation bulk under unipolar square waveform excitation is unavoidable even at high impulse repetition frequencies [16], [17]. In addition, at high frequency (up to 50 kHz) and fast rise time, the local electric field induced by interface space charge deposited through PD happening during previous impulse voltages plays an inevitable and crucial role in the behaviour of PD activity [18]. It should be noted that the space charge accumulation under unipolar repetitive impulse voltages was already proved in literature (e.g., [16]) through space charge measurements. Thus, space charge measurements are not performed in this work since the focus is mainly given to addressing the possible impact of space charge accumulation caused by unipolar excitations on the PD quantities (i.e., PDIV, PDEV, and RPDIV). The rate of changes in PD quantities under unipolar excitations as a function of exposure time should be clarified and addressed to help design experiments to obtain more meaningful and repeatable results. Therefore, this experimental study endeavours to evaluate the behaviours of PD quantities under unipolar impulsive voltage excitations as a function of exposure/poling time and how the pulse repetition frequency, rise time and excitation polarity affect the insulation performance. Indeed, by investigating the impact of space charge accumulation on PD activity, more accurate data/information is made available for the PD-free design of an inverter-fed machine when Type I insulated wire is employed. On the other hand, the variation rate of PDIV vs exposure time to a unipolar excitation for Type II insulated wire can provide an idea for better design of the electrical accelerated life tests in the presence of PD activity by applying a more exact over-voltage against PDIV as constant electrical ageing stress. Consequently, the potential consequences of space charge accumulation on the accelerated life tests can be considered, aiming to achieve a more exact electrical lifetime model.

Section II describes the test samples preparation, the PD measurement setup, and the test procedure. Then, section III analyzes the voltage excitation waveforms. Section IV explains the effect of space charge accumulation on electric field distribution. Section V reports and discusses the experimental results. Finally, section VI summarizes the main work conclusion.

II. METHODOLOGY

A. TEST SAMPLES

Two commercially available insulated wires are considered in the PD activity investigation. The first one is the Glass fibre insulated wire (2 Silix VSI) classified as Type II (mixed organic-inorganic) insulation, having a thermal index of 200°C. It is impregnated with silicone-based varnish manufactured by Von Roll. Its bare wire diameter and insulation thickness are 0.9 mm and 100 μm, respectively. Two Glass fibre insulated wires with a length of 22 cm are kept next to each other by a binding tape such as polytetrafluoroethylene (PTFE) to model the turn-to-turn insulation system in low voltage electrical machines [12]. Indeed, the two wires are not twisted to avoid the cracking of the Glass fibre coating during the twisting process. Therefore, PTFE tapes are used only to provide complete contact between the insulation surfaces of the two wires without being twisted (Fig. 1).

The second wire is PEEK insulated wire known as Type I (organic) insulation with a thermal index of 245°C manufactured by ZEUS. Its bare wire diameter and insulation thickness are 0.9 mm and 40 μm, respectively. According to the ASTM D2307 standard, the PEEK wires are twisted eight times under an applied tension weight of 1.35 kg (13.24 N). Fig. 1 illustrates the typical test samples: PTFE-wrapped pair

of Glass fibre insulated wires and twisted pair of PEEK insulated wires.

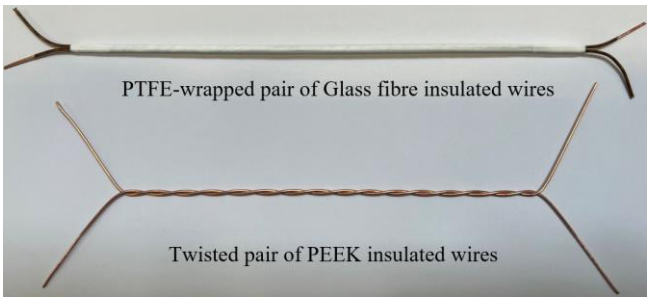

FIGURE 1. Test samples.

B. PD MEASUREMENT SETUP

Fig. 2 displays the schematic diagram of the PD measurement setup.

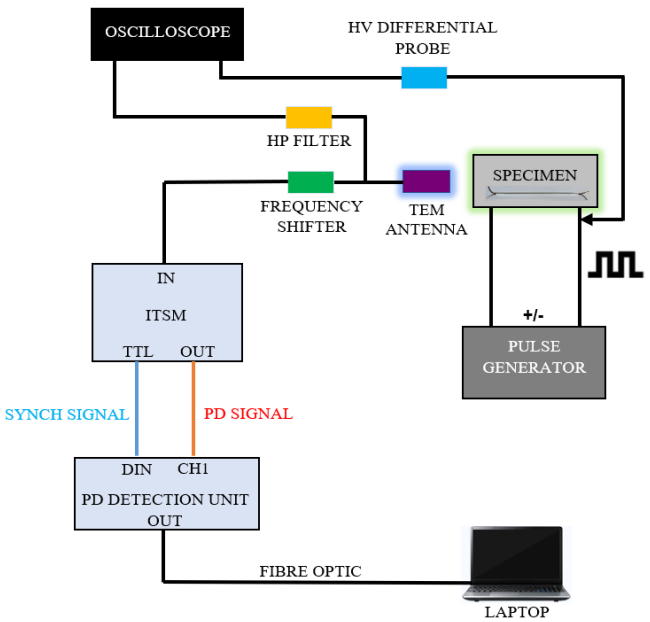

FIGURE 2. Circuit and connections layout for PD measurements setup.

The PD sensor is a high-frequency transverse electromagnetic antenna (TEM antenna) developed by Techimp and featuring the specifications listed in Table I [19]. It is placed at a distance of 15 cm from the specimen under test to get PD signals.

TABLE I
TEM ANTENNA SPECIFICATIONS

Bandwidth	100 MHz – 3 GHz
Gain	1.8 – 4.25 dBi
Voltage Standing Wave Ratio (VSWR)	5:1
3 dB Beam Width	100° - 210°
Polarization	linear
Impedance	50 Ω

The PD detection system is a Techimp PDBaseII. The PD detection unit has a bandwidth from 16 kHz up to 48 MHz and a sampling rate of 200 MSa/s [20]. The PD detection unit generates as output a pulse waveform for every detected PD and the minimum peak value triggering the PD signal detection and acquisition (i.e., PD trigger level) is set equal to 9 (mV).

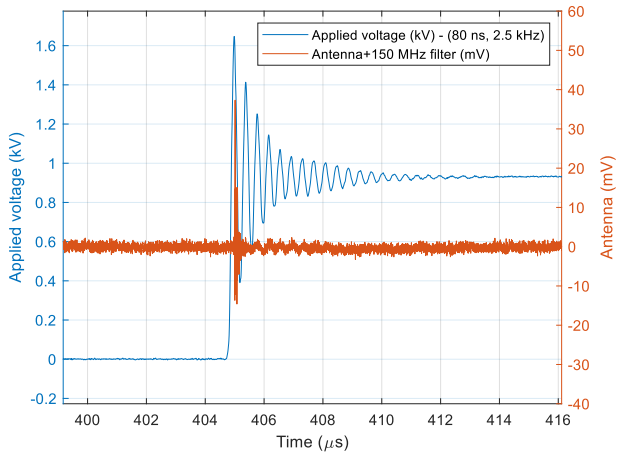

(a)

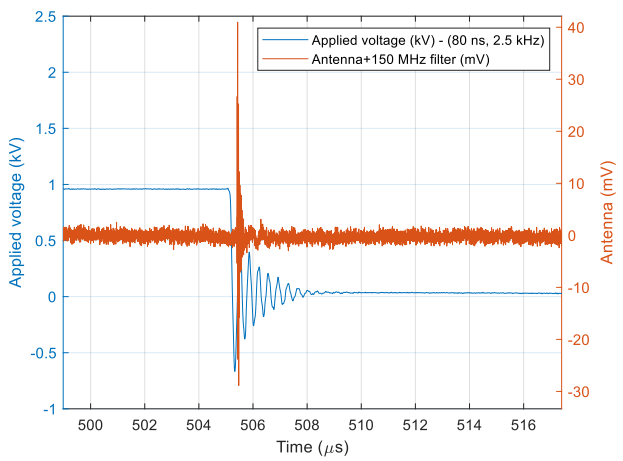

(b)

FIGURE 3. Typical captured PD signal by the TEM antenna and test waveform displayed by oscilloscope under positive unipolar repetitive impulse voltages (a) zoom-in rising edge, and (b) zoom-in falling edge.

Fig. 3 illustrates an example of a positive unipolar test waveform with 80 ns rise time, 2.5 kHz frequency and 1.65 peak magnitude (2.3 kV peak-to-peak) applied across the PTFE-wrapped pair of Glass fibre insulated wire. Fig. 3 shows the PD signal that occurred during the rising and falling edge; the zoom-in waveforms are depicted in Figs. 3a and 3b.

Figs. 4a and 4b depict the PD detection arrangement and test cell, respectively.

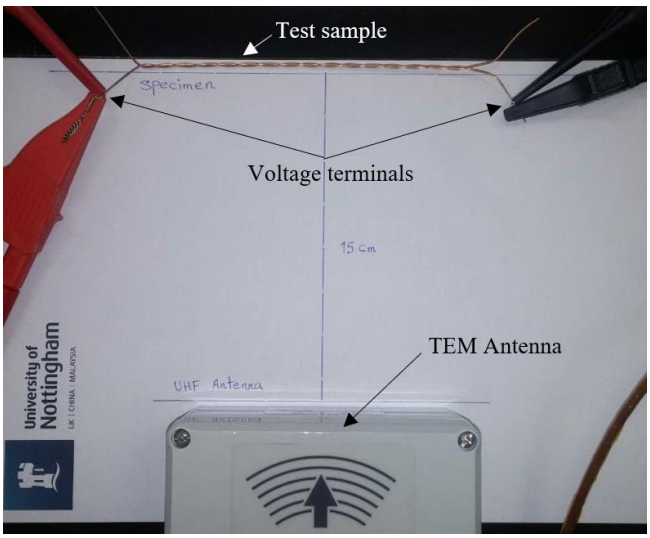

(a)

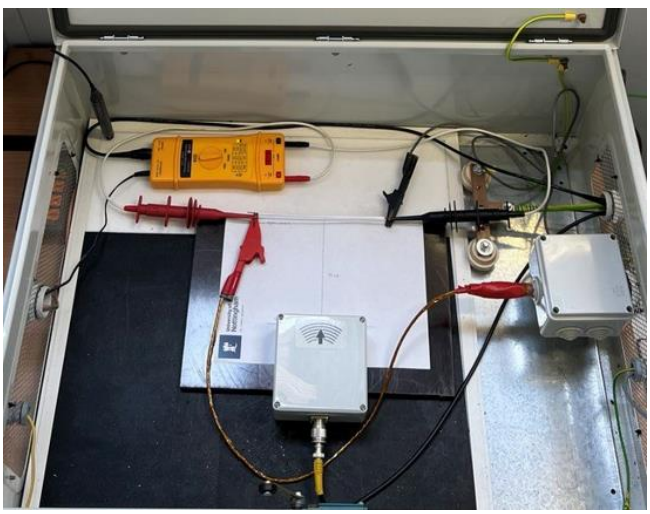

(b)

FIGURE 4. **(a) PD detection arrangement and (b) Test cell.**

A differential probe (50 MHz bandwidth, 2000:1 voltage ratio, 50 Ω impendence) measures the applied voltage across the specimen under test. A high-pass filter with a 150 MHz centre frequency is used to remove the pulse generator switching noise since PD signals have higher frequency contents than the commutation noise [18]. The voltage waveforms and PD signals are monitored by an oscilloscope (1 GHz bandwidth, 10 GS/s sampling rate). The oscilloscope is used to capture the PD signals with respect to the applied pulses to record the PD patterns. A 60 dB frequency shifter based on a peak envelope modulator is employed to match the high-frequency spectrum of the acquired signals to the lower frequency bandwidth of the PD detector. In addition, embedded high-pass filters in the frequency shifter help to reject the switching disturbances coming from the pulse generators to improve the Signal-to-Noise-Ratio (SNR). The impulsive test synchronization module (ITSM) produces a digital synchronization signal synchronized to the pulse generator's fundamental frequency through low pass filtering [21]. Therefore, the PD detection unit can perform PD tests under impulsive voltage excitations after switching disturbances rejection.

C. MEASUREMENT PROCEDURE

The PD tests are accomplished at room temperature (21°C), atmospheric pressure (1013 mbar) and relative humidity (28±5%). The positive and negative unipolar square voltage waveforms used for the PD tests are characterized by two pulse repetition frequencies (50 Hz and 2.5 kHz) and two rise times (80 and 800 ns). A lower frequency can promote space charge accumulation in the insulation bulk. On the other hand, a faster rise time can enhance the possibility of a higher surface charge caused by promoted PD charge magnitudes. The rise time is the rising edge portion at which the voltage increases from 0.1 to 0.9 of the peak value [22].

The pulse width duration is kept constant in all the test campaigns equal to 100 μs. The conceptual drawings of the excitation voltage waveforms with 100 μs constant pulse width are shown in Figs. 5a (50 Hz) and 5b (2.5 kHz). Since the pulse width is kept constant and two frequencies are tested, the two excitation voltages are characterized by different duty cycles, which are equal to 0.5% and 25% for 50 Hz and 2.5 kHz, respectively. It is worthwhile to mention that the variations of PDIV, PDEV and RPDIV as a function of the duty cycle are negligible for both measured peak and DC values [23]. In particular, a slight reduction in PD quantities (i.e., PDIV, PDEV and RPDIV) is observable for a shorter pulse impulse width [23]. Such a reduction is likely due to the availability of abundant starting electrons to initiate the avalanche, which occurs at a lower overvoltage [24].

The positive and negative unipolar excitations are generated by employing a commercial variable pulse generator system (RUP6-18bip). The polarity of the unipolar square waveform excitation can impact the PD quantities. For example, the measured PDIV under positive and negative polarity may not necessarily be the same [25]. For instance, Niemeyer [26] postulates that detrapping from a negatively charged surface is more difficult than detrapping from a positively charged surface.

The PD tests are performed without and with stressing/poling of the specimens. For the former (without poling), the voltage is increased in steps of 25 V peak every 30 seconds starting from a voltage level there is no PD activity. Once the PD is observed, the peak of the applied voltage is recorded as PDIV. Then, the voltage is reduced from PDIV in steps of 25 V peak every 1 minute to reach PDEV. The peak voltage is noted as PDEV when the PD activity stops. Eventually, the voltage increases from PDEV using the same voltage step and the stop duration as PDIV to trigger and measure RPDIV. When the PD activity occurs with a 50% probability of incepting a PD per voltage impulse, the peak voltage is recorded as RPDIV [11]. It is noteworthy to recall

that according to [11], RPDIV is the minimum peak-to-peak impulse voltage at which more than five PD pulses occur on ten voltage impulses of the same polarity.

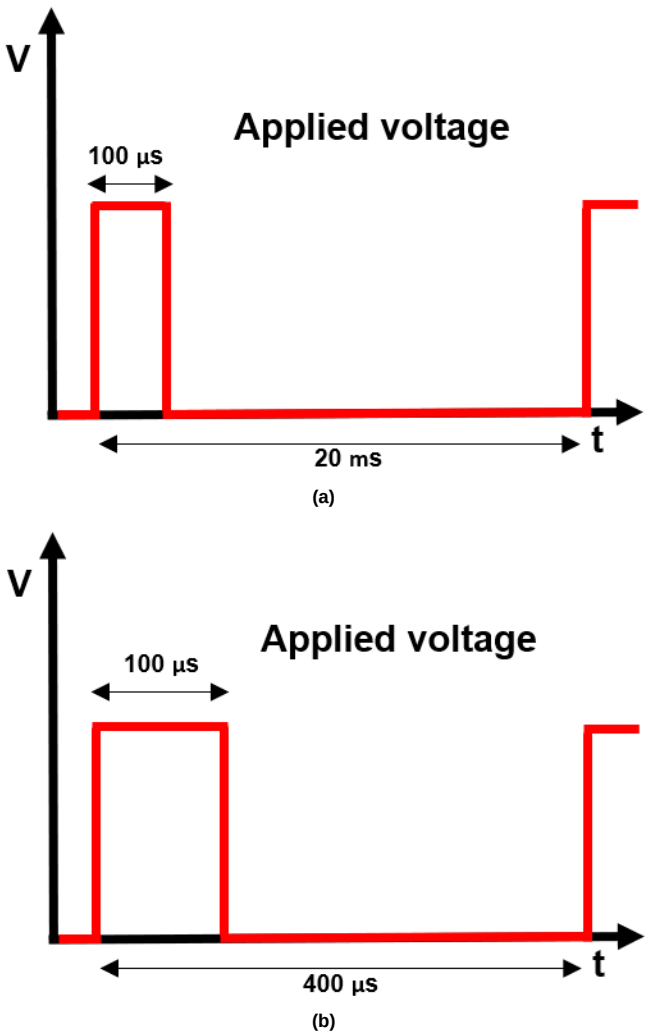

Figure 5. **Schematic diagrams of applied square waveforms excitations with the constant pulse width of 100 µs corresponding to (a) 50 Hz and (b) 2.5 kHz.**

The PD measurements are also carried out using pristine samples after stressing/poling the test samples. In this regard, first, PDIV is measured according to the described method. Then, the peak value of the applied voltage is reduced to 0.85×PDIV, i.e., as a constant poling voltage for two exposure time intervals: half an hour and one hour. The PDIV, PDEV and RPDIV are measured at the end of the poling times.

The PD quantities' measurement using the two approaches (i.e., with and without stressing/poling the samples) can reflect any possible inconsistency in the measured data caused by the space charge accumulation. In other words, more accurate data mirroring the PD quantities' variation range can support a more reliable PD-free design of inverter-fed machines and the design of experiments to achieve more congruous results.

In this paper, all the PD test results are reported based on peak value to provide a more direct comparison between the PD quantities (i.e., PDIV, PDEV and RPDIV). All the PD tests for each combination of poling time, voltage waveform and excitation polarity are performed using five fresh samples. Each specimen is tested only once to avoid the possibility of PDIV reduction due to damage resulting from previous PD activities [27].

In the following, it is explained why the measured peak value is preferred to the DC magnitude of the square waveforms. PDIV is the minimum measurable voltage at which PD can be incepted in the air gap/defect (i.e., V_{inc}). Both the peak value and DC magnitude of the steep-fronted voltage waveform excitations can be reported as PDIV. If the peak value is considered as a reference, the measured voltage is larger than V_{inc}. The opposite holds if the DC magnitude is recorded, giving a lower value than V_{inc} [28]. Recalling the two conditions which must be satisfied to trigger PD: (1) the voltage magnitude must exceed V_{inc}, and (2) a free electron must be available to initiate the avalanche. Consider Fig. 6, there are two voltage waveforms with equal DC amplitude, having different peak values/overshoots. If only the peak value reaches V_{inc} (dashed curve), PD cannot be incepted since only the first condition is satisfied. Indeed, the probability of the first electron availability is zero. If the peak value exceeds V_{inc} (solid curve), there is a possibility to have a first electron to incept PD in the shaded area [28]. Therefore, the peak value of the applied voltages is the distinguishing criterion between voltage waveforms with equal DC voltage magnitudes, having more impact on the measurable voltage as PDIV.

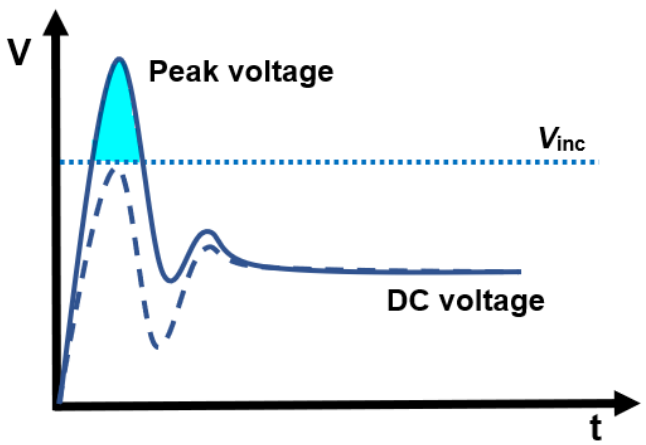

Figure 6. **Highlighting the impact of the peak value of the repetitive impulse voltages on the measurable voltage as PDIV.**

III. ANALYSIS OF VOLTAGE EXCITATION WAVEFORMS

A. WAVEFORMS IN TIME DOMAIN

The typical unipolar square waveform excitations with two pulse voltage repetition frequencies (i.e., 50 Hz and 2.5 kHz) and two rise time values (i.e., 80 and 800 ns) are illustrated in Fig. 7a.

The impact of different rise time values to deliver a constant DC voltage (e.g., 1 kV) is more evident in the zoom-in waveforms of the rising edge shown in Fig. 7b. As expected, the shorter rise time (i.e., 80 ns) leads to a significant overvoltage and ringing. As shown in Fig. 7, the impact of different pulse frequencies at a constant rise time (i.e., 80 ns) is not clear from the zoom-in waveforms in the time domain where the waveforms are almost overlapped (Fig. 7b).

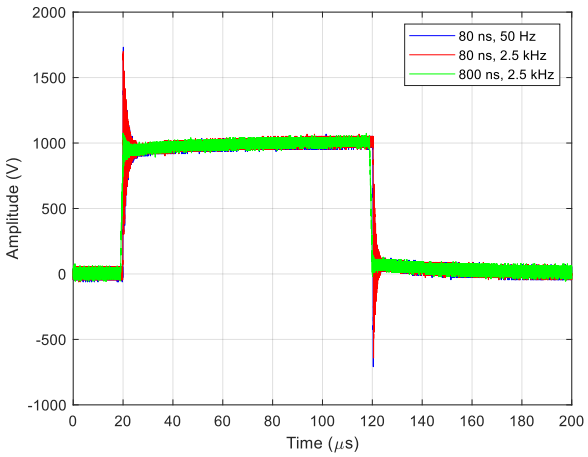

(a)

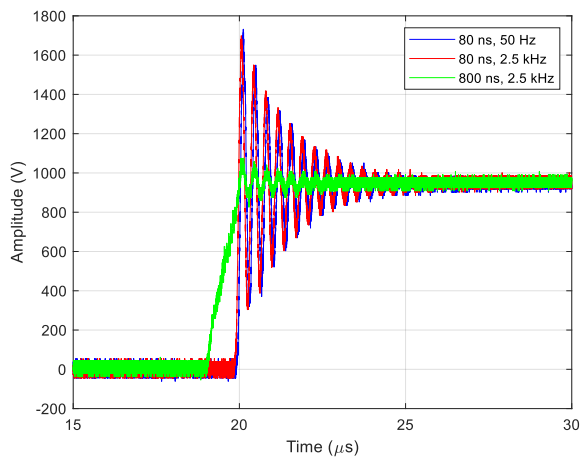

(b)

FIGURE 7. (a) The unipolar positive square wave excitations in time domain, and (b) zoom-in waveforms of the rising flanks.

B. WAVEFORMS IN FREQUENCY DOMAIN

The effects of switching frequency and rise time simultaneously can be demonstrated if referred to the frequency domain rather than the time domain. Therefore, Fig. 8 reports the Fast Fourier Transforms (FFT) of the three considered voltage waveforms (introduced in Fig. 7), corresponding to a time window equivalent to their relevant periodicity.

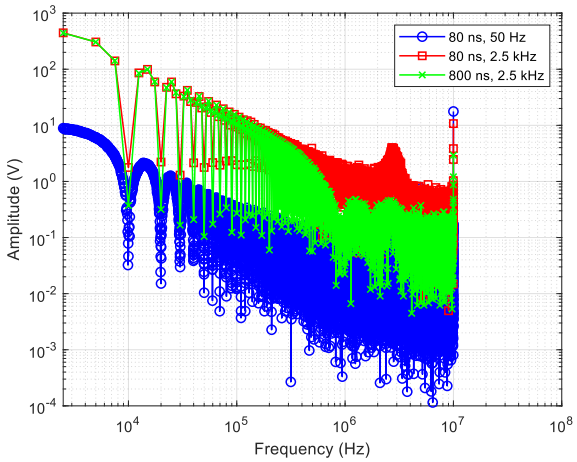

FIGURE 8. FFT of the unipolar square waveforms with two frequencies (50 Hz and 2.5 kHz) and two rise times (80 and 800 ns) at a constant DC voltage equal to 1 kV.

As shown in Fig. 8, the supply waveform spectral content depends on the pulse repetition frequency and rise time. At a constant rise time (i.e., 80 ns), an increase in pulse repetition frequency from 50 Hz to 2.5 kHz gives rise to the fundamental frequency of the waveform, shifting the harmonic distribution upward. However, at a constant pulse repetition frequency (i.e., 2.5 kHz), an increase in rise time from 80 to 800 ns reduces the energy content of the frequency spectrum. In other words, a shorter rise time leads to a higher frequency content, especially at frequencies of 2.7 MHz and 10 MHz.

The frequency spectrum analysis of the voltage waveforms applied to the samples is informative since the permittivity of the insulating materials can change with the spectral content of the supply waveform. Indeed, when the frequency content of the applied waveform to the insulation exceeds some critical frequency, f_c, the dipole orientation will not occur, resulting in permittivity reduction. The f_c is equal to the reverse of the relaxation time constant of the dipoles, τ, (i.e., $f_c=1/\tau$), where a dielectric loss peak appears [29]. As illustrated in Fig. 8 (the red spectrum), the highest spectral content of the waveform belongs to the case when both the pulse repetition frequency and the rise time are faster. This high-frequency content can result in a permittivity reduction, leading to a diminishment in the electric field enhancement factor in the air gap and eventually giving rise to the PDIV [18].

IV. EFFECT OF SPACE CHARGE ACCUMULATION ON ELECTRIC FIELD DISTRIBUTION

The permittivity rules mainly the electric field distribution under AC and pulse width modulation (PWM) excitations. In other words, the ratio of the relative permittivity of the dielectric to that of air primarily determines the electric field in the air gap. Since the relative permittivity of the insulation is higher than that of air trapped in the defect, the electric field in cavities embedded in the insulation is amplified compared to the distributed electric field in the solid insulation. Neglecting space charge accumulation in the

insulation bulk and interface, the electric field enhancement factor (i.e., f_E) of a spherical void embedded in solid insulation with a homogenous electric field distribution is delivered by (1) [30]:

$$f_E = \frac{E_c}{E_b} = \frac{\varepsilon_{rb}(f)}{1 + 2\varepsilon_{rb}(f)} \quad (1)$$

where $\varepsilon_{rb}(f)$ is the relative permittivity of the insulating material as a function of the frequency. E_c and E_b are the electric fields in the cavity and the insulation, respectively.

The electric field distribution can be affected by the space charge accumulation. It can occur through either or both interface space charge accumulation caused by PD activity and electrode injection inside insulation bulk. It is inevitable under unipolar excitations, even at high pulse repetition frequencies, due to the presence of a DC component [25], [31]. Then, the electric field in the air gap between the two insulated wires in the presence of space charge accumulation, E_c^*, is given by (2) [17]:

$$E_c^* = E_c + \frac{\rho \cdot \xi \cdot l_p + \sigma_s \cdot h_b}{\varepsilon_c \cdot h_b + \varepsilon_b(f) \cdot l_c} \quad (2)$$

where E_c is the electric field in the air gap between the two insulated wires in the absence of space charge accumulation. ρ is the charge per unit volume in the insulation bulk, and σ_s is the charge per surface unit at the interface. ξ is the thickness of charge packet, and l_p is the nearest distance between the charge packet and the conductor. The permittivity of insulation and medium filling between the two insulated wires (e.g., air) are expressed by $\varepsilon_b(f) = \varepsilon_0 \cdot \varepsilon_{rb}(f)$ and $\varepsilon_c = \varepsilon_0 \cdot \varepsilon_{rc}$, respectively, where ε_0 is the permittivity of free space ($8.85 \times 10^{-12} F/m$). ε_{rc} is the relative permittivity of the medium filling the cavity (for a gas-filled void, $\varepsilon_{rc} = 1$). h_b and l_c are the enamel insulation thickness and half of air gap length, respectively.

Equation (2) shows that when the polarity of ρ and σ_s is opposite of neighbouring electrode polarity (e.g., if ρ and $\sigma_s < 0$ accumulated near the positive electrode), the electric field in the air gap in the presence of space charge accumulation, E_c^*, becomes lower than the field in the absence of accumulated charge, E_c. Therefore, heterocharge space charge accumulation leads to a PDIV increase. The opposite happens for homocharge space charge accumulation, thus reducing PDIV [16].

A. INTERFACE SPACE CHARGE

The amount of interfacial space charge density, σ_s, can be expressed as:

$$\sigma_s = \sigma_{s1} \pm \sigma_{s2} \quad (3)$$

where the first term, σ_{s1}, is the interface charge trapping at the insulation/air interface when there is no PD event. It is calculated from the Maxwell equations at a steady state condition (thus, not changing with time) [32]. It is inevitably formed at the interface of two dielectrics having different conductivity and permittivity. The second term, σ_{s2}, is the interface charge resulting from the deposited charge due to PD activity. The initial amount of σ_{s2} depends directly on the PD charge magnitude, which can change through the charge decay mechanism. The surface charge decay/depletion time constant relevant to σ_{s2} corresponds to either or both charge diffusion/hopping into the dielectric bulk and charge recombination/neutralization rate along the defect surfaces [33]. A simplified approach to elucidate these processes is to deem that σ_{s2} decays through a simple first-order differential equation as in (4) [26]:

$$\sigma_{s2}(t) = \sigma_{s2}(t_0)\, exp(-\frac{t - t_0}{\tau}) \quad (4)$$

where τ is the decay time constant governing the charge decay process, t and t_0 are the current time and the time at which the last PD event happened, respectively. When the waveform characteristics such as rise time and pulse repetition frequency are faster than τ, the decay process cannot occur entirely under repetitive impulsive excitation (i.e., infinite memory effect). As a result, the non-decayed surface charge resulting from the PD activity, σ_{s2}, can influence the electric field intensity in the air gap. The typical range of charge decay time is 2–1000 ms [34]. The voltage pulse durations of the waveforms introduced in Figs. 7 and 8 are 20 ms and 400 µs associated with 50 Hz and 2.5 kHz, respectively. Consequently, the charge decay time can be longer than the voltage pulse duration, modifying the field distribution in the air gap and impacting PDIV.

In addition, a higher voltage slew rate (*dV/dt*) (i.e., a faster rise time) can also contribute to an increase in surface charge/interface space charge accumulation, σ_{s2}. Indeed, with a shorter rise time, PD charge magnitude increases [35], leading to an increase in surface charge density at the discharge point [25]. The last results in either or both easing the firing electron availability to initiate the discharge avalanche (thus, decrease of PDIV) and interface space charge accumulation impacting the field intensity in the air gap. The total interface charge, σ_s, beside the accumulated space charge in the insulation bulk, ρ, can increase or decrease the electric field in the air gap, acting as homocharge or heterocharge, respectively [17]. σ_{s1} and σ_{s2} can have an opposite or synergistic effect, making (3) such as $(\sigma_{s1} + \sigma_{s2})$ or $(\sigma_{s1} - \sigma_{s2})$ under heterocharge and homocharge accumulation, respectively, as illustrated in Fig. 9.

B. A SIMPLIFIED VISUAL MODEL

Fig. 9 depicts a simplified model for the electric field behaviour in the air gap in the presence of PD activity under unipolar positive repetitive square wave excitation, showing electrode, insulation, and spherical cavity. Fig. 9 shows that there is homocharge accumulation during (a) rising edge, (b) falling edge (close to zero crossing), and (c) rest time (end of pulse duration). (a′), (b′) and (c′) are relevant cases to (a), (b) and (c), respectively, when there is heterocharge

accumulation. E_{sc1} is the field due to the space charge accumulation. E_{q2} is the local field resulting from the surface charge deposited by PD, E_0 is the geometric background field and E is the resulting field in the cavity.

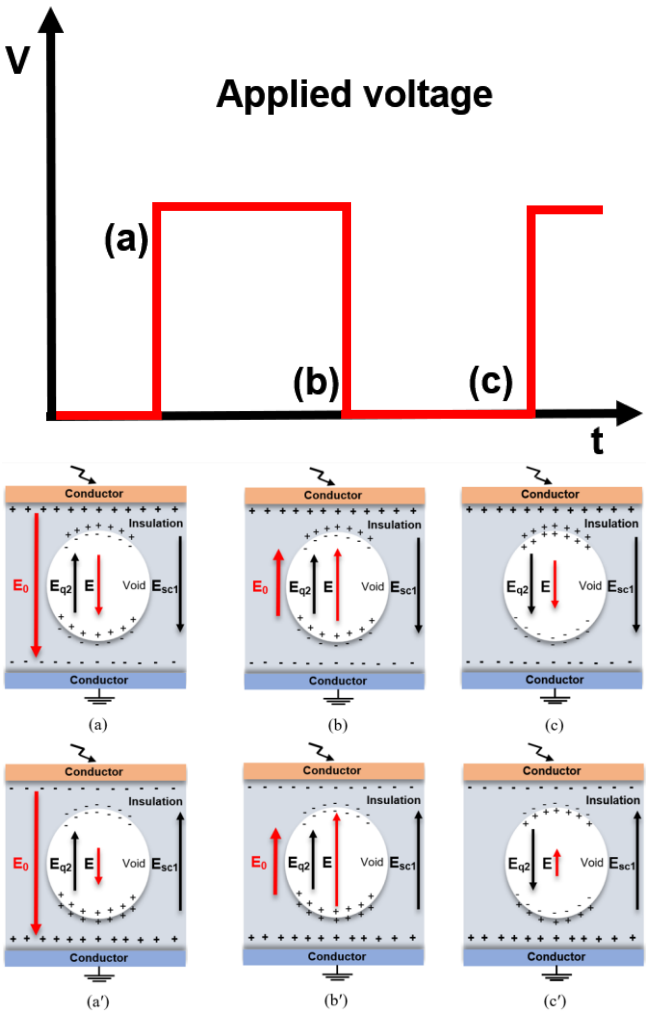

FIGURE 9. A simplified model for the electric field variations in the air gap in the presence of PD activity under unipolar positive repetitive square wave excitations.

This demonstration gives a clear visual insight into the electric field variation in an internal defect or an air gap between two insulated wires. Indeed, the electric field can be affected by space charge accumulation in the air/insulation interface, insulation bulk and the surface charge deposited through subsequent PD activity.

The assumptions made for analyzing Fig. 9 are:

- The voltage impulse duration and *dV/dt* (i.e., rise time) are much faster than the required time for the deposited charge by the subsequent PD, σ_{s2}, to decay. Therefore, the model relies on the assumption of infinite memory effect so that the field originated by the deposited charge inside the air gap (i.e., the local electric field, E_{q2}) would not decrease between PD events [36].
- The space charge accumulation in the air/insulation interface, σ_{s1}, and in the insulation bulk, ρ, are in the steady state condition [32].
- The field excursion during the falling edge after the zero crossing exceeds the PD inception field. Therefore, PD can occur even if the applied external voltage is zero, resulting in incepting PD and reversing E_{q2} vector direction [17].

Fig. 9 shows that the local electric field, E_{q2}, caused by the deposited surface charge through subsequent PD, σ_{s2}, reduces and increases the electric field during the rising and falling edges, respectively. Therefore, when the space charge accumulation is neglected (i.e., $\sigma_{s1} = 0$ and $\rho = 0$, thus $E_{sc1} = 0$), the resulting electric field is estimated as:

$$E = f_E \cdot E_0 \pm E_{q2} \tag{5}$$

where f_E is the electric field enhancement factor, assuming the space charge accumulation is neglected, can be approximated from (1) for a spherical void. $+E_{q2}$ and $-E_{q2}$ are considered in (5) for falling and rising edges, respectively.

The electric field, E_{sc1}, caused by the homocharge space charge accumulation (i.e., $\sigma_{s1} > 0$ and $\rho > 0$), increases and decreases the electric field during the rising and falling flanks, respectively. The opposite holds for the heterocharge space charge accumulation (i.e., $\sigma_{s1} < 0$ and $\rho < 0$).

Hence, (5) can be modified in the presence of space charge accumulation as:

$$E = f'_E \cdot E_0 \pm E_{q2} \pm E_{sc1} \tag{6}$$

where f'_E is the field amplification factor when the space charge is accumulated. For homocharge, $+E_{sc1}$ and $-E_{sc1}$ are considered in (6) during rising and falling flanks, respectively, holding the reverse for the heterocharge. However, the impact of E_{sc1} on the electric field in the air gap and PDIV is negligible under bipolar excitations having pulse repetition frequencies higher than 10 Hz [16]. As a result, the increase of electric field in the air gap caused by the accumulated homocharge during rising edge or heterocharge during falling edge leads to a lower peak-to-peak value of PDIV under unipolar impulse voltages than those obtained at bipolar ones at atmospheric pressure (1013 mbar) [15]. Fig. 9 shows that when there is a heterocharge space charge accumulation, the maximum electric field in the air gap is most likely ascribed to the falling edge, determining the PDIV (Fig. 9b′). In the case of homocharge accumulation, the maximum electric field can occur during either rising or falling edges, depending on the values of E_{q2} and E_{sc1}. Additionally, the comparison between Figs. 9c and 9c′ show that the electric field in the air gap at the end of pulse duration is higher when there is homocharge accumulation than heterocharge.

The total amount of interfacial space charge density, σ_s, is affected by the polarity of the interface space charge accumulation, σ_{s1}, being homocharge or heterocharge. In the case of homocharge, the recombination/neutralization can

occur easier due to the reaction between σ_{s1} and σ_{s2}, having different polarities, and then (3) becomes $\sigma_s = \sigma_{s1} - \sigma_{s2}$. However, the opposite holds for the case of heterocharge where σ_{s1} and σ_{s2} have the same polarity giving rise to the total surface charge, then (3) delivers $\sigma_s = \sigma_{s1} + \sigma_{s2}$.

Considering only the rising edges, PDIV can decrease and increase by homocharge and heterocharge space charge accumulation, respectively [25]. Therefore, the impact of the prevailing mechanism on PD activity is a topic worthy of being experimentally investigated. In the next section, the possible effect of space charge accumulation on PD quantities: partial discharge inception voltage (PDIV), partial discharge extinction voltage (PDEV) and repetitive partial discharge inception voltage (RPDIV) caused by positive and negative unipolar excitations for two types of wire insulations as a function of exposure time are compared and investigated experimentally.

V. EXPERIMENTAL RESULTS AND DISCUSSIONS

The measurement results as a function of poling time are presented and plotted using boxplots to provide a clear visual insight. Each box plot is obtained from testing five fresh samples and summarizes a data set by illustrating the median value, q_2 (central line in the box), the 25th, q_1, and 75th, q_3, percentiles (the edge of the box), the data range (using whiskers at q_2-1.5×(q_3-q_1) and q_2+1.5×(q_3-q_1)). The symbols outside the whiskers show outliers. The small square symbol inside each box denotes the mean value [37].

A. PDIV VS EXPOSURE/POLING TIME

Figs. 10 and 11 display the measured peak values of PDIV versus exposure time for the Glass fibre and PEEK insulated wires, respectively. Tables II and III show the mean values of PDIV corresponding to Figs. 10 and 11, respectively. The measurements are carried out under six unipolar square waveform excitations: three waveforms as shown in Fig. 7, both positive and negative polarities. During the poling time, an excitation voltage waveform featuring the same parameters (i.e., polarity, frequency and rise time) as that considered at zero poling time, is applied to the samples.

1) GLASS FIBRE INSULATED WIRES

Fig. 10 (left) indicates that under positive excitation, there is a slight decrease in PDIV after one hour (e.g., a mean reduction of 90 V), likely due to the homocharge space charge accumulation, increasing the electric field in the air gap (Fig. 9a), resulting in a PDIV drop. However, under negative polarity, the continuous heterocharge or interfacial polarization can diminish the electric field in the defect, giving rise to the PDIV by 210 V [17]. These results confirm the different behaviour of PDIV for the Glass fibre insulated wire as a function of poling time under positive and negative excitations when the rise time and pulse repetition frequency are 80 ns and 50 Hz, respectively.

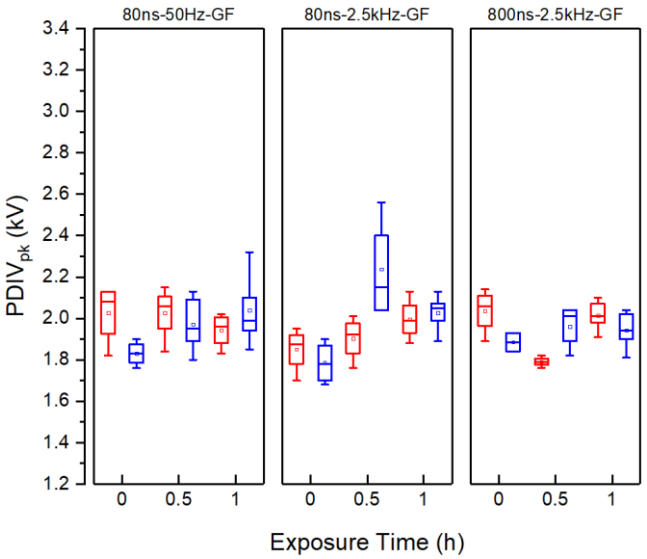

FIGURE 10. PDIV vs poling time in Glass fibre insulated wire at two different frequencies and rise times for unipolar positive (red plot) and negative (blue plot) pulse voltage excitations (poling voltage = 0.85 PDIV). Each box plot is obtained from testing five fresh samples.

TABLE II
THE MEAN VALUES OF PDIV RELEVANT TO FIG. 10

Exp. Time (h)	80 ns, 50 Hz		80 ns, 2.5 kHz		800 ns, 2.5 kHz	
	PDIV$_{pk}$ (kV)					
	Pos.	Neg.	Pos.	Neg.	Pos.	Neg.
0	2.03	1.83	1.85	1.79	2.04	1.89
0.5	2.03	1.97	1.9	2.24	1.79	1.96
1	1.94	2.04	2	2.03	2.01	1.94

Fig. 10 (middle) shows that under positive polarity at 2.5 kHz, there is a gradual increase of PDIV as a function of exposure time (i.e., a mean increase of 150 V after one hour of poling). It is likely due to less time for the heterointerface charge resulting from subsequent PD to decay (Fig. 9a′), mitigating the electric field in the defect [31]. The lowest PDIV occurs before stressing the Glass fibre insulated wire, regardless of the excitation polarity [38].

Fig. 10 (middle) illustrates that PDIV initially rises by 450 V during the first half of exposure time under negative excitation, likely due to the opposite contribution of heterocharge accumulation/interfacial polarization (prevailing) and homocharge accumulation. Moreover, a faster rise time (e.g., 80 ns) probably gives rise to the hetero-interfacial space charge. It can also lead to a higher PDIV than a longer rise time (i.e., 800 ns, Fig. 10 right) after half an hour, delivering 110 and 280 V higher PDIV at 80 ns than 800 ns under positive and negative polarity, respectively. After a longer poling time (i.e., one hour), PDIV decreases by 210 V under negative excitations at 80 ns and 2.5 kHz, showing almost the same value as the measured one at 50 Hz. It is probably because of homocharge space charge accumulation in insulation bulk, ρ, prevailing over the impact of surface charge/interface space charge, σ_s, as time increases. Indeed, when the frequency rises under negative excitations, the results show different time constants for

heterocharge/interfacial polarization and homocharge accumulation, which is shorter for the former at 2.5 kHz, delivering a non-monotone trend for PDIV as a function of poling time [16]. As a result, the highest difference between the results at 50 Hz and 2.5 kHz is 270 V, observed after half an hour under negative excitation. The impact of pulse repetition frequency on PDIV becomes negligible at a longer time (e.g., one hour), especially under negative excitation (comparing Fig. 10 left and middle), likely due to the impact of space charge accumulation in the insulation bulk of Glass fibre, predominating as time increases.

Fig. 10 (right) illustrates that when rise time is longer under positive excitation, there is an initial PDIV decrement by 250 V, giving a minimum value of 1.79 kV after half an hour. It is probably because a shorter time constant of the homocharge accumulation (Fig. 9a) initially prevails. However, after half an hour, there is an almost stable PDIV under negative excitation. Indeed, PDIV varies lower for a longer rise time (800 ns) versus exposure time. It is likely due to less influence of surface charge in the electric field modification since a longer rise gives a lower surface charge density [23], [25]. Considering the results demonstrated in Fig. 10, the variation rate of PDIV as a function of poling time is the highest when the rise time is the fastest (i.e., 80 ns) and pulse repetition frequency is the highest (i.e., 2.5 kHz). While the former increases interfacial space charge accumulation through PD charge magnitude promotion [39], the latter gives less time for decaying deposited charges caused by subsequent PD. Consequently, σ_s can modify the electric field between the enamelled wires before prevailing the space charge accumulation in the insulation bulk, ρ, at a longer poling time.

Regarding the impact of rise time on PDIV (comparing Fig. 10 middle and right), it is interesting to highlight that a faster rise time (i.e., 80 ns) delivers a lower PDIV before stressing the specimens (i.e., 190 V and 100 V smaller than 800 ns for positive and negative polarity, respectively) [23]. After one hour of exposure time, when space charge accumulation in the insulation bulk dominates, PDIV for different rise time values becomes comparable, regardless of the excitation polarity [38].

For the Glass fibre insulated wire, the PDIV under positive polarity is always higher than the PDIV under negative excitation before stressing the samples (i.e., $PDIV^+ > PDIV^-$) [23]. However, it is not the case after stressing the samples.

2) PEEK INSULATED WIRES

Fig. 11 and Table III manifest the lowest PDIV for the PEEK insulated wires measured before stressing the specimen in all cases. Indeed, PDIV increases after stressing the PEEK, most likely due to an inherent propensity of PEEK for the heterocharge accumulation under unipolar excitation, resulting in an electric field reduction in the air gap (Fig. 9a′). PDIV under negative polarity is lower than positive excitation when the pulse repetition frequency is lower (i.e., 50 Hz), independent of the exposure time. The negative excitation gives a 470 V PDIV decrement after one hour when the space charge accumulation in the insulation bulk can dominate.

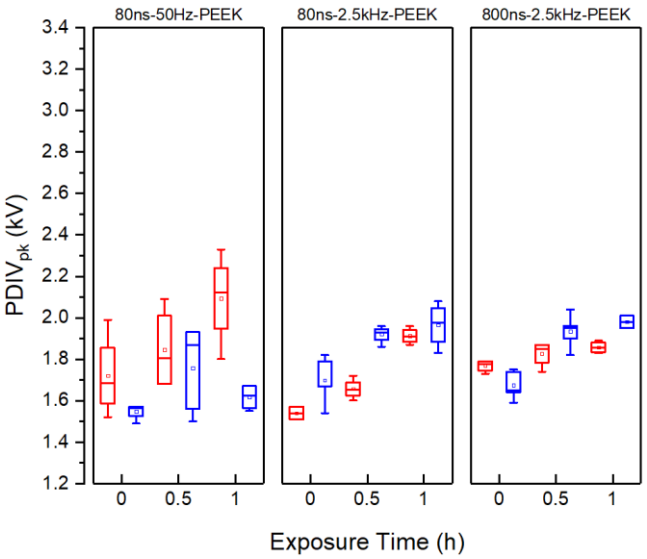

FIGURE 11. PDIV vs poling time in PEEK insulated wire at two different frequencies and rise times for unipolar positive (red plot) and negative (blue plot) pulse voltage excitations (poling voltage = 0.85 PDIV). Each box plot is obtained from testing five fresh samples.

TABLE III
THE MEAN VALUES OF PDIV RELEVANT TO FIG. 11

Exp. Time (h)	80 ns, 50 Hz		80 ns, 2.5 kHz		800 ns, 2.5 kHz	
	$PDIV_{pk}$ (kV)					
	Pos.	Neg.	Pos.	Neg.	Pos.	Neg.
0	1.72	1.55	1.54	1.7	1.77	1.67
0.5	1.85	1.76	1.66	1.92	1.83	1.93
1	2.09	1.62	1.91	1.97	1.86	1.98

The comparison between Fig. 11 (left) and (middle) demonstrates that the impact of increasing frequency from 50 Hz to 2.5 kHz is different under positive and negative excitations. Under positive polarity, frequency increase diminishes PDIV, likely due to the synergistic impact of homocharge accumulation and higher first electron availability caused by more surface charge density, prevailing the effect of permittivity reduction. However, the reverse holds for the negative excitation where frequency increase gives rise to PDIV. It can be ascribed to the synergistic effect of permittivity reduction and heterocharge accumulation (Fig. 9a′), reducing the field in the defect. Interestingly, the measured PDIV under positive and negative excitations are comparable at 80 ns and 2.5 kHz after a longer poling time (e.g., one hour). It is the opposite of a lower frequency (i.e., 50 Hz), where the space charge accumulation in the insulation bulk is more plausible [16], [17].

Fig. 11 (right) and Table III display that although before poling the PEEK insulated wire, measured PDIV under positive excitation is 100 V higher than the negative one, the reverse holds after stressing the specimens. It is likely due to a higher heterocharge accumulation in the insulation bulk under negative polarity [38].

The comparison between Fig. 11 (middle) and (right) represents the impact of rise time on PDIV as a function of poling time. It illustrates that a higher slew rate gives 230 and 170 V lower PDIV before stressing the PEEK insulated wire and after half an hour of poling under positive excitation. However, PDIV becomes comparable at 80 and 800 ns under positive polarity when poling time is longer (i.e., one hour). It can be due to electric field reduction owing to heterointerface charge caused by faster rise time featuring a higher time constant than homocharge accumulation. However, under negative excitation and after stressing the specimen, there is almost independency of PDIV on the rise time referring to the mean and median values. At a higher pulse repetition frequency (i.e., 2.5 kHz), the PDIV under negative excitation is higher than the positive one after stressing the specimens regardless of the rise time. However, the polarity dependence of PDIV changes as a function of rise time before poling the samples. For example, at a faster rise time (i.e., 80 ns), PDIV is 160 V higher under negative excitation, while manifesting a 100 V PDIV increase at a longer rise time (i.e., 800 ns) under positive excitation.

It is noteworthy to highlight that a shorter rise time (e.g., 80 ns) delivers a lower PDIV before stressing the PEEK insulated wires under unipolar excitations regardless of its polarity, referring to the lower whisker, thus the lowest percentile [38]. It means that neither permittivity reduction due to the high spectral frequency content (Fig. 8) nor the low probability of having a starting electron to initiate PD when the rise time is the shortest cannot explain this phenomenon [40]. Indeed, as *dV/dt* increases, there is less time for surface charge decay [18]. It can accelerate the firing electron harvesting process, predominating over other factors, resulting in a lower PDIV. These explanations are also valid for Glass fibre insulated wire (Fig. 10), referring to either a selected percentile in the tail of the distribution or mean/median values for both polarities.

3) GLASS FIBRE VS PEEK INSULATED WIRES

The two wire topologies comparison reveals that Glass fibre gives a higher PDIV in most cases. It is due to the larger insulation thickness of Glass fibre being decisive since the PDIV sensitivity on permittivity is less than insulation thickness and the restricted range of permittivity variation among different materials [14], [41]. Interestingly, there is one exceptional case in which the PEEK insulated wire can give 150 V higher PDIV, although it has a smaller insulation thickness. This case occurs when poling time is longer (e.g., one hour) at (80 ns, 50 Hz) under positive excitation. It is probably due to the heterocharge accumulation in the bulk of PEEK, prevailing over other factors, diminishing the electric field in the air gap. As a result, the PDIV data spotlight that the impact of space charge accumulation on the PDIV tests under unipolar excitation is inevitable.

B. PDEV VS EXPOSURE/POLING TIME

When the voltage reduces with respect to PDIV, there is still PD activity for the initial decreasing steps. Although the geometric background field decreases, the resulting internal electric field in the air gap remains higher than the inception field, and PD is incepted. Firstly, it is likely due to the electric field from the space charge deposited by a discharge added to the geometric background field during the falling flanks, providing a higher electric field than the inception field. Secondly, this surface charge can accelerate the firing electron harvesting process to start PD (thus, the two conditions to incept PD can still be fulfilled). It can occur more probably during the falling edges of the square wave excitations (Figs. 9b and 9b′).

1) GLASS FIBRE INSULATED WIRES

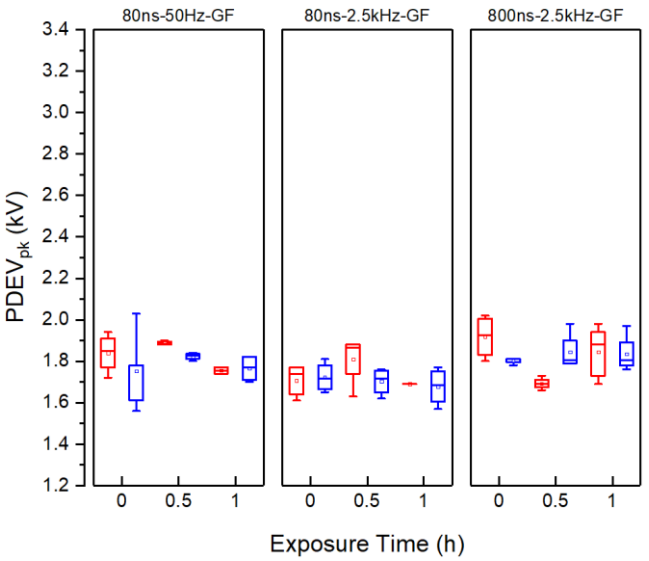

FIGURE 12. PDEV vs poling time in Glass fibre insulated wire at two different frequencies and rise times for unipolar positive (red plot) and negative (blue plot) pulse voltage excitations (poling voltage = 0.85 PDIV). Each box plot is obtained from testing five fresh samples.

TABLE IV
THE MEAN VALUES OF PDEV RELEVANT TO FIG. 12

Exp. Time (h)	80 ns, 50 Hz		80 ns, 2.5 kHz		800 ns, 2.5 kHz	
	PDEV$_{pk}$ (kV)					
	Pos.	Neg.	Pos.	Neg.	Pos.	Neg.
0	1.84	1.75	1.71	1.72	1.92	1.8
0.5	1.89	1.82	1.81	1.7	1.69	1.85
1	1.76	1.77	1.69	1.68	1.84	1.84

Interestingly, Fig. 12 and Table IV manifest an almost polarity independence for PDEV of Glass fibre insulated wires after a longer exposure time (i.e., one hour) for all the considered excitation waveforms, referring to the mean value. It can be due to the accumulated space charge in the insulation bulk dominating over the interface space charge.

Fig. 12 (left) and (middle) illustrate that after increasing the pulse repetition frequency from 50 Hz to 2.5 kHz, the measured PDEV decreases for all the exposure times regardless of the excitation polarity. For instance, PDEV reduction is 130 V under positive polarity before stressing the samples. It is most likely due to the less time for the deposited charge from the subsequent PD to decay at a higher frequency

for the Glass fibre insulated wire. The voltage pulse duration at 2.5 kHz is 400 µs. It is much shorter than the required time for surface charge decay which is 2-1000 ms [34]. The surface charge left by the PD acts as a source of initial electrons, considering the Schottky-Richardson emission mechanism. Indeed, the electrons released by the surface overcome those caused by the background radiation, resulting in a lower PDEV at a higher pulse repetition frequency [34], [24].

Comparing Figs. 12 (middle) and (right) demonstrates the impact of rise time on the PDEV. It shows that a faster rise time (i.e., 80 ns) delivers a lower PDEV in most cases [23]. It is likely due to a shorter rise time giving less time for the surface charge decay, making the PDEV lower [38].

2) PEEK INSULATED WIRES

Fig. 13 (left) indicates an almost polarity independence for the PDEV of PEEK insulated wires before stressing the specimens. However, the measured PDEV under positive excitation is 240 and 370 V higher after half an hour and one hour of poling the samples, respectively (same trend as PDIV). It is probably due to the electric field reduction in the air gap resulting from the interface charge [31]. The behaviour of PDEV is non-monotone under negative polarity consequent to the exposure time (same trend as PDIV). It is possibly due to a longer time constant of the homocharge accumulation in the insulation bulk prevailing over the impact of interface charge after a longer poling time (i.e., one hour).

Fig. 13 (middle) and Table V display that when both the rise time and frequency are the fastest, there is an increasing trend for PDEV as a function of exposure time, while the measured PDEV under negative excitation is higher (same trend as PDIV). This increase can be attributed to the electric field mitigation in the air gap owing to the heterocharge interface space charge accumulation or interfacial polarization as a function of exposure time.

The comparison between Fig. 13 (left) and (middle) reveals the impact of frequency on the PDEV of the PEEK insulated wire. It demonstrates that a different excitation polarity reflects a diverse frequency impact on PDEV. A higher frequency gives a lower PDEV under positive polarity, referring to the mean and median values, especially after stressing the specimens. However, the opposite holds for the negative polarity, where a lower pulse repetition frequency delivers a lower PDEV, especially after a longer poling time (i.e., 310 V lower PDEV).

Fig. 13 (right) represents that when the rise time becomes longer (i.e., 800 ns), the variation rate of PDEV decreases [38]. The PDEV shows the same trend as PDIV as a function of exposure time indicated in Fig. 11 (right). PDEV under negative polarity is 100 V lower than positive one. However, the opposite holds after stressing the specimens for one hour when PDEV under negative excitation is 160 V larger. It is possibly due to the homocharge and heterocharge accumulation in the insulation bulk after a longer poling time under positive and negative excitations, respectively.

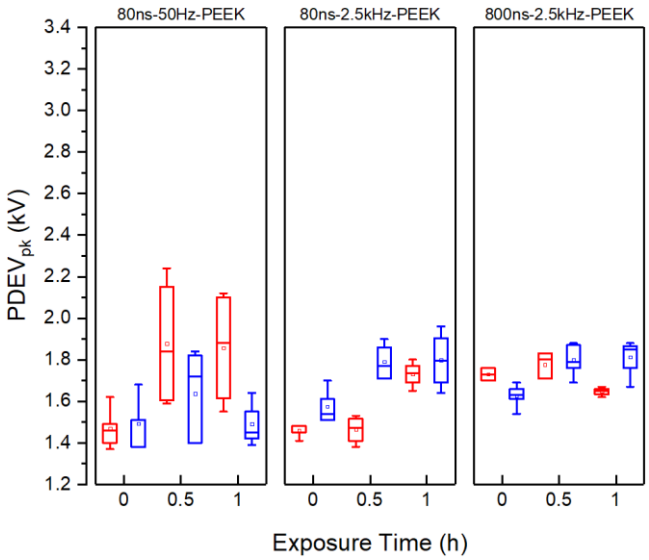

FIGURE 13. PDEV vs poling time in PEEK insulated wire at two different frequencies and rise times for unipolar positive (red plot) and negative (blue plot) pulse voltage excitations (poling voltage = 0.85 PDIV). Each box plot is obtained from testing five fresh samples.

TABLE V
THE MEAN VALUES OF PDEV RELEVANT TO FIG. 13

Exp. Time (h)	80 ns, 50 Hz		80 ns, 2.5 kHz		800 ns, 2.5 kHz	
	PDEV$_{pk}$ (kV)					
	Pos.	Neg.	Pos.	Neg.	Pos.	Neg.
0	1.47	1.49	1.46	1.57	1.73	1.63
0.5	1.88	1.64	1.46	1.79	1.78	1.8
1	1.86	1.49	1.73	1.8	1.65	1.81

Comparing Fig. 13 (middle) and (right) indicate the impact of rise time on the PDEV as a function of poling time. Referring to the mean and median values, it shows that a lower PDEV of PEEK insulated wire belongs to a shorter rise time (i.e., 80 ns) before stressing the samples (same as PDIV) [38]. For example, PDEV is 270 V lower at 80 ns under positive polarity. It verifies the previous observation for the Glass fibre (Fig. 12), where there is a lower PDEV for a shorter rise time before poling. The PDEV of a faster rise time (i.e., 80 ns) can reach only 60 V higher than that of a longer rise time (i.e., 800 ns) after stressing the specimens for a longer poling time (i.e., one hour) under positive excitation. However, there is almost comparable PDEV for faster and longer rise times under negative polarity and after stressing the samples.

3) GLASS FIBRE VS PEEK INSULATED WIRES

Comparing the two insulated wires indicates that Glass fibre delivers a higher PDEV before stressing the samples. It can be ascribed to its larger insulation thickness, while the permittivity of the magnet wires does not differ significantly. At a lower pulse repetition frequency (50 Hz) and under positive excitation, the PEEK insulated wire shows a higher variation of PDEV after stressing the specimens. The rate of change is such that the measured PDEV of PEEK can be higher than the Glass fibre, referring to the upper whisker (thus, a higher percentile). This high variation rate is likely due to the longer voltage pulse duration of the waveform at 50 Hz

(i.e., 20 ms), being in the range of charge decay time for the deposited charge caused by PD (i.e., 2–1000 ms). As a result, the PDEV of the PEEK insulated wire is affected by the surface charge at 50 Hz after stressing under positive excitation. This point should be considered in planning tests to compare the insulated wires with different insulation thicknesses by selecting proper test waveforms. It is noteworthy to highlight that when both rise time and frequency are faster (i.e., 80 ns and 2.5 kHz), the PDEV of Glass fibre becomes 120 V lower than that of PEEK after a longer exposure time (i.e., one hour) under negative polarity. It is most likely due to the impact of high surface charge left by the PD, owing to a higher voltage slew rate and frequency for the Glass fibre. It can accelerate the firing electron harvesting process, helping to keep alive the PD activity at a lower geometric background field based on the Schottky-Richardson emission mechanism [24], [34].

C. RPDIV VS EXPOSURE/POLING TIME

RPDIV can be affected more than PDIV by the surface charge density/interface space charge accumulation at the discharge point owing to a higher deposited charge from the subsequent PD events under RPDIV. It is due to more PD repetition rate for RPDIV than PDIV.

1) GLASS FIBRE INSULATED WIRES

As illustrated in Fig. 14 (left), RPDIV shows a considerable initial decrement by 570 V at 50 Hz during the first half of poling time under positive excitation, which may be due to the homocharge accumulation on air/insulation interfaces. After a longer poling time (i.e., one hour), there is an increase of 310 V in RPDIV, likely due to the accumulated heterocharge in insulation bulk, prevailing as time increases. Like PDIV (Fig. 10 left), the RPDIV under positive excitation is notably higher than the negative polarity (i.e., 530 V larger) before stressing the specimens. Interestingly, this polarity dependence becomes less tangible after poling samples when space charge accumulation stabilises. The trends of RPDIV and PDIV of Glass fibre at 50 Hz as a function of exposure time are the same under negative excitation, giving a 340 V higher value after a longer poling time (i.e., one hour).

When pulse repetition frequency increases from 50 Hz to 2.5 kHz (Fig. 14 middle), RPDIV decreases obviously for all cases regardless of the exposure time. Under positive polarity, this RPDIV decrement is remarkable before stressing the samples (i.e., 820 V) and after one hour of exposure time (i.e., 680 V). This RPDIV drop is considerable under negative excitation. For instance, RPDIV is 530 V and 700 V lower at 2.5 kHz sequentially before stressing the samples and after one hour of poling. It is ascribed to the less time for the surface charge decay, giving rise at a higher frequency acting as a source for the firing electron generation, resulting in RPDIV reduction. After stressing the Glass fibre, RPDIV under negative excitation is 270 V higher, particularly after the first half of poling time (same as PDIV). It is worthwhile to highlight that the polarity dependence of RPDIV is lower after a longer exposure time, probably due to space charge accumulation in the insulation bulk, predominating over other factors. Although the behaviour of RPDIV consequent to poling time is the same as PDIV under negative excitation (i.e., showing an initial increase followed by a reduction), the reversed trends hold under positive polarity. It means that while RPDIV decreases by 120 V as a function of poling time under positive excitation, PDIV increases by 150 V. It is most likely due to interface homocharge accumulation which is more plausible under RPDIV due to its higher PD repetition rate. However, the accumulated heterocharge in the insulation bulk is decisive under PDIV and positive excitation.

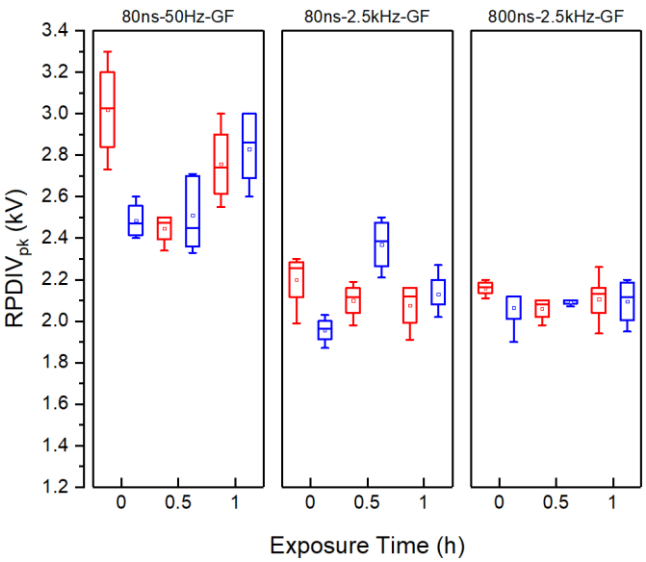

FIGURE 14. RPDIV vs poling time in Glass fibre insulated wire at two different frequencies and rise times for unipolar positive (red plot) and negative (blue plot) pulse voltage excitations (poling voltage = 0.85 PDIV). Each box plot is obtained from testing five fresh samples.

TABLE VI
THE MEAN VALUES OF RPDIV RELEVANT TO FIG. 14

Exp. Time (h)	80 ns, 50 Hz		80 ns, 2.5 kHz		800 ns, 2.5 kHz	
	RPDIV$_{pk}$ (kV)					
	Pos.	Neg.	Pos.	Neg.	Pos.	Neg.
0	3.02	2.49	2.2	1.96	2.16	2.07
0.5	2.45	2.51	2.1	2.37	2.06	2.09
1	2.76	2.83	2.08	2.13	2.11	2.1

Interestingly, when the rise time increases to 800 ns (Fig. 14 right), there is less variation of RPDIV as a function of poling time, especially under negative excitation referring to the mean value. It spotlights the importance of interface space charge impact on RPDIV. Indeed, with a longer rise time, PD charge magnitude decreases [35], leading to a lower surface charge density at the discharge point than the faster rise time [25], resulting in a lower change in RPDIV consequent to the exposure time.

The comparison between RPDIV results at (80 ns, 2.5 kHz) and (800 ns, 2.5 kHz) can reflect the impact of rise time on RPDIV of Glass fibre insulated wires. The influence of rise time on RPDIV under negative excitation is the same as PDIV, showing a lower and higher RPDIV at a faster rise time before

and after stressing the Glass fibre insulated wires, respectively. After the first half of poling time, a higher RPDIV associated with a shorter rise time is more evident, especially under negative excitation (i.e., 280 V larger at 80 ns). Indeed, the heterocharge interface charge impact probably predominates over the effect of homocharge accumulation after half an hour when the rise time is faster. The latter can overcome the former after a longer poling time (i.e., one hour), resulting in less impact of rise time observed for both excitation polarities. The reason to have a lower RPDIV at a faster rise time before stressing the specimens under negative excitation is likely the less time for the surface charge decay when the rise time is shorter. In this case, a higher surface charge at the discharge point can increase the firing electron generation, combined with more oscillations/ringing when the rise time is faster (Fig. 7b), when the instantaneous voltage can exceed the RPDIV for a longer time, resulting in lower measured RPDIV values at a shorter rise time [42]. The same holds for the positive excitation (i.e., before stressing), referring to a lower percentile of RPDIV. The comparison between Figs. 14 (right) and 11 (right) shows that the polarity dependence of RPDIV and PDIV as a function of poling time is the same when the rise time is longer (i.e., 800 ns). It is likely due to less surface charge left by PD events under RPDIV at a longer rise time.

2) PEEK INSULATED WIRES

Fig. 15 (left) displays that the measured RPDIV for PEEK insulated wire at 50 Hz is higher under positive excitation than the negative one after stressing the samples like PDIV results (Fig. 11 left). The RPDIV is 230 V and 430 V higher under positive polarity after half an hour and one hour, respectively. However, RPDIV is 270 V higher under negative polarity before poling the PEEK. The trend of RPDIV as a function of poling time is non-monotone for both excitation polarities. Indeed, there is an initial increase during the first half of exposure time which can be attributed to the interfacial polarization or heterocharge interface space charge accumulation. The comparison between the trend of PDIV and RPDIV can reflect the effect of higher interface space charge accumulation which is more plausible under RPDIV. For instance, although PDIV increases monotone under positive excitation, there is a reduction of RPDIV by 270 V after one hour of exposure time. It is likely due to the opposite contribution of interface accumulated heterocharge (prevailing) and homocharge accumulation in the insulation bulk, which would be dominated after a longer poling time. However, the behaviour of RPDIV and PDIV of PEEK as a function of exposure time is similar at 50 Hz and under negative polarity. When the pulse repetition frequency is increased from 50 Hz to 2.5 kHz (Fig. 15 middle), RPDIV of PEEK decreases under positive excitation regardless of the poling time. This RPDIV drop is considerable (i.e., 800 V) after half an hour of poling. Under negative polarity, there is 210 V of RPDIV decrement before stressing the PEEK. Indeed, the firing electron availability increases due to a higher surface charge left by PD at a higher frequency, predominating over the impact of permittivity reduction at a higher frequency.

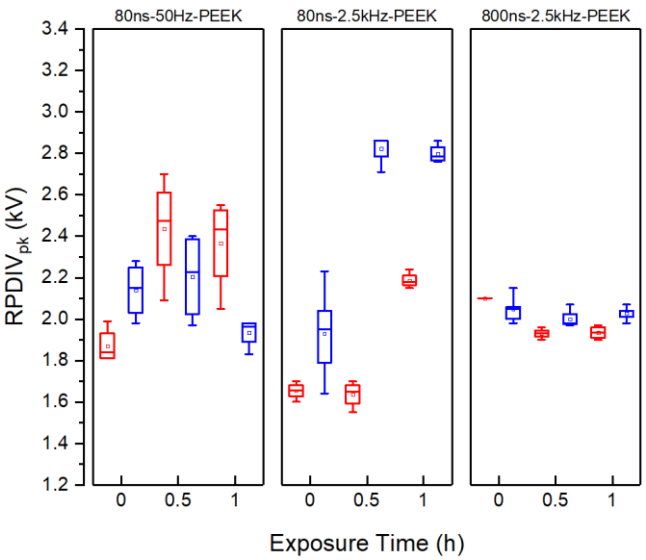

FIGURE 15. RPDIV vs poling time in PEEK insulated wire at two different frequencies and rise times for unipolar positive (red plot) and negative (blue plot) pulse voltage excitations (poling voltage = 0.85 PDIV). Each box plot is obtained from testing five fresh samples.

TABLE VII
THE MEAN VALUE OF RPDIV RELEVANT TO FIG. 15

Exp. Time (h)	80 ns, 50 Hz		80 ns, 2.5 kHz		800 ns, 2.5 kHz	
	$RPDIV_{pk}$ (kV)					
	Pos.	Neg.	Pos.	Neg.	Pos.	Neg.
0	1.87	2.14	1.65	1.93	2.1	2.05
0.5	2.44	2.21	1.64	2.82	1.93	2
1	2.37	1.94	2.19	2.8	1.94	2.03

However, under negative excitation, when the pulse repetition frequency is increased to 2.5 kHz (Fig. 15 middle), the RPDIV of PEEK tends to be significantly higher than those measured at 50 Hz (Fig. 15 left) after poling of samples. The RPDIV at 2.5 kHz is 610 V and 860 V larger than 50 Hz after half an hour and one hour of excitation, respectively. It is most likely due to the synergistic effect of permittivity reduction and heterointerface space charge accumulation, resulting in this substantial electric field reduction in the air gap, prevailing over the impact of higher surface charge left by PD at (80 ns, 2.5 kHz) and eventually giving rise to RPDIV. All the PD quantities (i.e., PDIV, PDEV and RPDIV) of PEEK stabilize after the first half of poling time at 80 ns and 2.5 kHz under negative excitation, which can be attributed to the heterocharge space charge accumulation in the insulation bulk. Additionally, the notable increase of RPDIV compared with PDIV under negative excitation at (80 ns, 2.5 kHz) can be associated with the heterocharge interface space charge accumulation, which is more likely to occur under RPDIV rather than PDIV. However, RPDIV remains almost stable during the first half of poling, followed by a considerable increase (i.e., 550 V) after a longer poling time under positive polarity. The RPDIV enhancement is probably because of accumulated heterocharge in the insulation bulk, being

observed under negative excitation with a higher value. The polarity dependency of RPDIV of PEEK as a function of poling time at (80 ns, 2.5 kHz) is the same as the PDIV, where the measured values are remarkably higher under the negative excitation, especially after stressing the PEEK. For example, RPDIV is 1.18 kV higher under negative polarity than the positive one after half an hour of poling at 80 ns and 2.5 kHz.

The comparison between the results at (80 ns, 2.5 kHz) and (800 ns, 2.5 kHz) can reflect the effect of rise time on RPDIV of PEEK insulated wires as a function of poling time and excitation polarity. Fig. 15 and Table VII illustrate that under both unipolar excitations (like PDIV), a lower RPDIV belongs to the faster rise time (i.e., 80 ns) before poling the PEEK insulated wires. For example, the RPDIV is 450 V and 120 V lower at 80 ns than 800 ns under positive and negative excitation, respectively. The RPDIV is also 290 V lower at 80 ns than 800 ns after poling PEEK for half an hour under unipolar positive excitation. The reasons mentioned explaining a lower RPDIV at a faster rise time before stressing the specimens for Glass fibre (i.e., more surface charge density and oscillations at a shorter rise time) are valid for the PEEK.

However, a faster rise time can deliver a higher RPDIV for PEEK under negative excitation after poling and under positive polarity after a longer poling time (i.e., one hour). Under negative excitation, RPDIV is 820 V and 770 V larger at 80 ns than 800 ns after half an hour and one hour of poling, respectively. It is most likely due to the synergistic impact of heterocharge interface space charge accumulation caused by faster rise time (since observed after poling the specimens), combined with a higher probability of having a starting electron less affected by its inherent delay when the rise time is longer (i.e., 800 ns), leading to RPDIV reduction. Moreover, an increase in rise time from 80 ns to 800 ns decreases the energy content of the frequency spectrum of the voltage waveform (Fig. 8 green plot), resulting in a higher permittivity than a faster rise time, an electric field increase in the air gap, and eventually RPDIV decrement at a longer rise time (i.e., 800 ns).

Fig. 15 (right) shows that the RPDIV variations as a function of poling time at a longer rise time (i.e., 800 ns) are negligible.

3) GLASS FIBRE VS PEEK INSULATED WIRES

The comparison between the Glass fibre and PEEK insulated wire at 50 Hz represents that Glass fibre gives a significantly higher RPDIV than PEEK under negative excitation (i.e., 890 V larger) after one hour of poling time (same trend as PDIV). It is also valid under positive polarity, referring to a lower whisker, thus a lower percentile of RPDIV. Comparing the two insulated wires at (800 ns, 2.5 kHz) shows that Glass fibre gives a higher RPDIV for all cases, referring to the mean values (Tables VI and VII). A higher RPDIV of Glass fibre is ascribed to its larger insulation thickness considering the limited range of permittivity values in the magnet wires [14], [41].

It is worthwhile to highlight that the remarkable RPDIV enhancement of PEEK at 80 ns and 2.5 kHz after poling, most likely due to the synergistic impact of permittivity drop and heterocharge accumulation can result in a higher RPDIV for PEEK than the Glass fibre insulated wire, which has thicker insulation. For instance, the RPDIV of PEEK under negative excitation is 450 V and 670 V higher than Glass fibre after half an hour and one hour of poling, respectively. Under positive polarity, PEEK also can give 110 V larger RPDIV after one hour of exposure time.

Interestingly, the impact of poling time on RPDIV becomes almost negligible when the rise time increases from 80 ns to 800 ns for both insulated wires, most probably due to lower surface charge density at the discharge point when the rise time is longer.

D. RPDIV AND PDIV DISPERSSION LEVEL

The dispersion levels of measurement results are quantified, relying on the shape/slope parameter of the 2-parameter Weibull distribution as (7) [43], [44]:

$$F(V_{\mathrm{PD}}) = 1 - \exp\left[-\left(\frac{V_{\mathrm{PD}}}{\alpha}\right)^{\beta}\right] \tag{7}$$

where V_{PD} corresponds to the measured PDIV or RPDIV values. α and β are scale and shape/slope parameters, respectively. α corresponds to the PD quantities at a cumulative probability of 63.2%, and the β is attributed to the data dispersion of each data set.

The PDIV and RPDIV measurement dispersion levels are determined and quantified for each test condition by testing five pristine specimens and fitting the data to (7) using the median ranks method, calculated by the inverse of the incomplete beta function [14]. The shape/slope parameter (i.e., β) of the Weibull distribution is a dimensionless parameter being used to summarize the dispersion level of the collected data for each case study. Fig. 16 shows the difference between the RPDIV and PDIV dispersion levels relevant to the RPDIV data reported in (Figs. 14 and 15) and the PDIV data in (Figs. 10 and 11), as a function of poling time.

Fig. 16 indicates that $(\beta_{\mathrm{RPDIV}} - \beta_{\mathrm{PDIV}})$ almost decreases as a function of exposure time, delivering $(\beta_{\mathrm{RPDIV}} \approx \beta_{\mathrm{PDIV}})$ after a longer poling time, especially under positive excitation. This finding is helpful for PD diagnostics. The reason for this convergence is that as poling time increases, the effect of space charge accumulation in the insulation bulk becomes predominated over the impact of interface space charge accumulation. The latter can be made more under RPDIV than PDIV since the PD repetition rate is higher under RPDIV.

Therefore, the impact of interface space charge can be more decisive before stressing the specimens under RPDIV. When the interface charge is homocharge, it can give rise to the electric field in the air gap, exceeding the PD inception field [17]. In addition, surface charge left by the PD can act as a source for firing electrons to initiate PD [24], especially from a positively charged surface where detrapping is inherently

easier than detrapping from a negatively charged surface (due to a minor surface work function for the earlier) [26]. As a result, the firing electron emission rate can be higher under RPDIV before stressing the samples, resulting in less dispersion for RPDIV (i.e., $\beta_{\mathrm{RPDIV}} > \beta_{\mathrm{PDIV}}$). Indeed, $(\beta_{\mathrm{RPDIV}} - \beta_{\mathrm{PDIV}})$ can reflect the impact of surface charge left by PD on the emission rate of firing electrons. It can be perceived from Fig. 16 that the increasing effect of surface charge on the acceleration of firing electron emission rate decreases as a function of poling time. This reduction is more for the PEEK insulated wire under positive excitation at (800 ns, 2.5 kHz). However, when the rise time is faster (i.e., 80 ns), the surface charge can be higher due to less time for the surface charge decay. It can not necessarily result in higher β under RPDIV. As shown in Fig. 16, under positive excitation and at (80 ns, 2.5 kHz) for PEEK, the dispersion level of RPDIV is higher than PDIV regardless of the exposure time (i.e., $\beta_{\mathrm{PDIV}} > \beta_{\mathrm{RPDIV}}$). Indeed, when the rise time is faster, the PD charge amplitude is higher [18], [37], resulting in more deposited charge due to PD. On the other hand, a higher voltage slew rate leads to higher PD charge magnitude dispersion caused by the first electron availability delay [39], leading to more scattering in the deposited charge. As a result, a more variable surface charge density impacts the electric field and the firing electron emission rate, resulting in more dispersion under RPDIV, eventually, $(\beta_{\mathrm{PDIV}} > \beta_{\mathrm{RPDIV}})$ when the rise time is shorter.

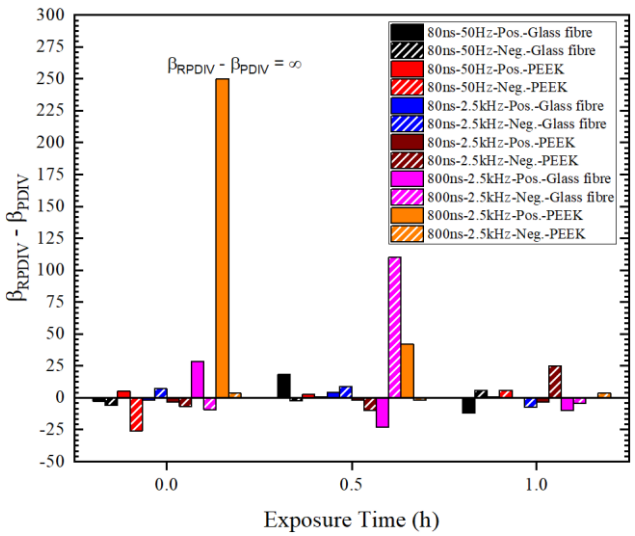

FIGURE 16. The difference between RPDIV and PDIV dispersion levels as a function of poling time under unipolar positive and negative pulse voltage excitations, relying on the shape/slope parameter of the Weibull distribution.

There are also some cases where $(\beta_{\mathrm{RPDIV}} > \beta_{\mathrm{PDIV}})$ after a longer poling time (i.e., one hour), such as PEEK insulated wire at (80 ns, 2.5 kHz) under negative excitation. These are the cases where the high surface charge caused by a faster rise time prevails over other factors, providing a higher electric field than PD inception and a high emission rate for the firing electron to initiate PD. Indeed, in these conditions, the surface charge is high, and surface charge decay at trapping sites is low. It predominates over the higher surface work function under negative excitation, giving rise to the firing electron emission rate to initiate PD even after a longer poling time. Therefore, all the mentioned players can overcome or synergize the impact of space charge accumulation in the insulation bulk after a longer poling time.

VI. CONCLUSIONS

This article demonstrates that the possible impact of space charge accumulation (especially interface charge) under unipolar steep-fronted square wave excitations must be considered in planning tests to reach more repeatable and congruous results. The experimental results at atmospheric pressure (1013 mbar) show that the plausible level of interface charge and its impact on the PD quantities can depend on pulse repetition frequency and rise time, changing as a function of exposure time. The effect of interface charge is speculated to be substantial for RPDIV at a faster rise time and frequency. In this case, the insulated wires, even with a smaller insulation thickness (e.g., PEEK), can deliver a considerably higher RPDIV than the wires with a larger insulation thickness (e.g., Glass fibre) after a longer poling time. Therefore, the poling time can be assimilated to the service hour of the motor, linking the PD investigation results to a practical application. However, RPDIV at a longer rise time has less variation as a function of poling time. The data post-processing reveals that after a longer poling time (thus, space charge stability in the insulation bulk), the dispersion levels of PDIV and RPDIV become comparable (i.e., $\beta_{\mathrm{RPDIV}} \approx \beta_{\mathrm{PDIV}}$), which is a benefit in PD diagnostics.

REFERENCES

[1] A. Cavallini, D. Fabiani and G. C. Montanari, "Power electronics and electrical insulation systems - part 1: phenomenology overview," IEEE Electr. Insul. Mag., vol. 26, no. 3, pp. 7-15, May-June 2010.
[2] G. Stone, S. Campbell, and S. Tetreault, "Inverter-fed drives: which motor stators are at risk?," IEEE Industry Applications Magazine, vol. 6, no. 5, pp. 17-22, Sept.-Oct. 2000.
[3] J. Millan, P. Godignon, X. Perpina, A. Perez-Tomas, and J. Rebollo, "A survey of wide bandgap power semiconductor devices," IEEE Trans. Power Electron., vol. 29, no. 5, pp. 2155–2163, 2014.
[4] U.S. Department of Energy, "Chapter 6: innovating clean energy technologies in advanced manufacturing, wide bandgap semiconductors for power electronics technology assessment," Quadrennial Technol. Rev., 2015.
[5] R. Singh and S. Sundaresan, "Fulfilling the promise of high-temperature operation with silicon carbide devices: eliminating bulky thermal-management systems with SJTs," IEEE Power Electron. Mag., vol. 2, no. 1, pp. 27–35, 2015.
[6] M. Ghassemi, "Accelerated insulation aging due to fast, repetitive voltages: A review identifying challenges and future research needs," IEEE Trans. Dielectr. Electr. Insul., vol. 26, no. 5, pp. 1558-1568, Oct. 2019.
[7] M. Kaufhold, G. Borner, M. Eberhardt, and J. Speck, "Failure mechanism of the interturn insulation of low voltage electric machines fed by pulse-controlled inverters," IEEE Electr. Insul. Mag., vol. 12, no. 5, pp. 9–16, Sep. 1996.
[8] A. Cavallini, D. Fabiani and G. C. Montanari, "Power electronics and electrical insulation systems - part 2: life modeling for insulation design," IEEE Electr. Insul. Mag., vol. 26, no. 4, pp. 33-39, July-Aug. 2010.

[9] M. Galea, P. Giangrande, V. Madonna and G. Buticchi, "Reliability-oriented design of electrical machines: the design process for machines' insulation systems must evolve," IEEE Industrial Electronics Magazine, vol. 14, no. 1, pp. 20-28, Mar. 2020.
[10] A. Rumi, J. Marinelli and A. Cavallini, "Dielectric Characterization of Impregnating Varnishes for Inverter-Fed Motors," 2022 IEEE 4th International Conference on Dielectrics (ICD), 2022, pp. 389-392.
[11] IEC 60034-18-41, Rotating electrical machines - Part 18-41: Partial discharge free electrical insulation systems (Type I) used in rotating electrical machines fed from voltage converters - Qualification and quality control tests, 2014.
[12] IEC 60034-18-42, Rotating electrical machines - Part 18-42: Qualification and acceptance tests for partial discharge resistant electrical insulation systems (Type II) used in rotating electrical machines fed from voltage converters, 2016.
[13] P. Wang, G. C. Montanari and A. Cavallini, "Partial discharge phenomenology and induced aging behavior in rotating machines controlled by power electronics," IEEE Transactions on Industrial Electronics, vol. 61, no. 12, pp. 7105-7112, Dec. 2014.
[14] A. Rumi, J. G. Marinelli, D. Barater, A. Cavallini and P. Seri, "The challenges of reliable dielectrics in modern aerospace applications: the hazard of Corona Resistant materials.," IEEE Trans. Transp. Electrific., 2022.
[15] Peng Wang, Hongying Xu, Jian Wang, Wanya Zhou and A. Cavallini, "The influence of repetitive square wave voltage rise time on partial discharge inception voltage," 2016 IEEE Conference on Electrical Insulation and Dielectric Phenomena (CEIDP), Toronto, ON, Canada, 2016, pp. 759-762.
[16] D. Fabiani, G. C. Montanari, A. Cavallini and G. Mazzanti, "Relation between space charge accumulation and partial discharge activity in enameled wires under PWM-like voltage waveforms," IEEE Trans. Dielectr. Electr. Insul., vol. 11, no. 3, pp. 393-405, June 2004.
[17] Cavallini, D. Fabiani and G. C. Montanari, "Power electronics and electrical insulation systems - Part 3: Diagnostic properties," IEEE Electr. Insul. Mag., vol. 26, no. 5, pp. 30-40, Sept.-Oct. 2010.
[18] Z. Guo, A. Q. Huang, R. E. Hebner, G. C. Montanari and X. Feng, "Characterization of partial discharges in high-frequency transformer under PWM pulses," IEEE Transactions on Power Electronics, vol. 37, no. 9, pp. 11199-11208, Sept. 2022.
[19] TEM Antenna Datasheet. Accessed: Jan. 7, 2023. [Online]. Available: https://www.altanova-group.com/en/products/partial-discharge-tests/sensors-and-accessories/tem-antenna.
[20] A. Contin, A. Cavallini, G. C. Montanari, G. Pasini, and F. Puletti, "Digital detection and fuzzy classification of partial discharge signals," IEEE Trans. Dielectr. Electr. Insul., vol. 9, no. 3, pp. 335–348, Jun. 2002.
[21] L. Fornasari, A. Caprara and G. C. Montanari, "Partial discharge measurements in electrical machines controlled by variable speed drives: from design validation to permanent PD monitoring," 9th IEEE International Symposium on Diagnostics for Electric Machines, Power Electronics and Drives (SDEMPED), pp. 384-390, Aug. 2013.
[22] N. Driendl, F. Pauli, and K. Hameyer, "Modeling of partial discharge processes in winding insulation of low-voltage electrical machines supplied by high du/dt inverters," IECON 2019 - 45th Annual Conference of the IEEE Industrial Electronics Society, Lisbon, Portugal, 2019, pp. 7102-7107.
[23] H. Naderiallaf, P. Giangrande and M. Galea, "Investigating the effect of waveform characteristics on PDEV, PDIV and RPDIV for Glass fibre insulated wire," 2022 International Conference on Electrical Machines (ICEM), 2022, pp. 1327-1333.
[24] P. Wang, H. Xu, J. Wang, W. Wang and A. Cavallini, "Effect of repetitive impulsive voltage duty cycle on partial discharge features and insulation endurance of enameled wires for inverter-fed low voltage machines," IEEE Trans. Dielec. Elec. Insul., vol. 24, no. 4, pp. 2123-2131, 2017.
[25] H. Naderiallaf, P. Giangrande and M. Galea, "A contribution to thermal ageing assessment of Glass fibre insulated wire based on partial discharges activity," IEEE Access, vol. 10, pp. 41186-41200, 2022.
[26] L. Niemeyer, "A generalize approach to partial discharge modeling," IEEE Trans. Dielect. Electron. Insul., vol. 2, no. 4, pp. 510–528, Aug. 1995.
[27] M. Goldman, A. Goldman and J. Gatellet, "Physical and chemical aspects of partial discharges and their effects on materials," 1993 International Conference on Partial Discharge, 1993, pp. 11-14.
[28] L. Lusuardi, A. Rumi, A. Cavallini, D. Barater and S. Nuzzo, "Partial Discharge Phenomena in Electrical Machines for the More Electrical Aircraft. Part II: Impact of Reduced Pressures and Wide Bandgap Devices," IEEE Access, vol. 9, pp. 27485-27495, 2021.
[29] A. Rumi, A. Cavallini and L. Lusuardi, "Impact of WBG Converter Voltage Rise-Time and Switching Frequency on the PDIV of Twisted Pairs," 2020 IEEE 3rd International Conference on Dielectrics (ICD), Valencia, Spain, 2020, pp. 902-905.
[30] H. Edin, "Partial discharges studied with variable frequency of the applied voltage," Ph.D. dissertation, KTH, Stockholm, Sweden, 2001.
[31] M. Takashima, K. Soda and T. Takada, ''Measurement of electric charges at the interface between two dielectric layers using an electro-acoustic transducer technique'', IEEE Trans. Electr. Insul., Vol. 23, pp. 287-295, 1988.
[32] T. Jing, Surface charge accumulation in SF6, Ph.D. Thesis, Delft University Press, Delft, The Netherlands, 1993.
[33] C. Abadie, T. Billard, and T. Lebey, "Partial discharges in motor fed by inverter: From detection to winding configuration," IEEE Trans. Ind. Appl., vol. 55, no. 2, pp. 1332–1341, Mar./Apr. 2019.
[34] F. Gutfleisch and L. Niemeyer, "Measurement and simulation of PD in epoxy voids," IEEE Trans. Dielect. Elect. Insul., vol. 2, no. 5, pp. 729–743, Oct. 1995.
[35] P. Wang, A. Cavallini and G. C. Montanari, "Characteristics of PD under square wave voltages and their influence on motor insulation endurance," IEEE Trans. Dielec. Elec. Insul., vol. 22, no. 6, pp. 3079-3086, December 2015.
[36] P. Seri, H. Naderiallaf and G. C. Montanari, "Modelling of supply voltage frequency effect on partial discharge repetition rate and charge amplitude from AC to DC at room temperature," IEEE Trans. Dielec. Elec. Insul., vol. 27, no. 3, pp. 764-772, June 2020.
[37] P. Wang, A. Cavallini, G. C. Montanari and G. Wu, "Effect of rise time on PD pulse features under repetitive square wave voltages," IEEE Trans. Dielec. Elec. Insul., vol. 20, no. 1, pp. 245-254, February 2013.
[38] H. Naderiallaf, P. Giangrande and M. Galea, "Experimental considerations on the possible impact of space charge accumulation on partial discharges activity for wire insulations," 2022 IEEE 4th International Conference on Dielectrics (ICD), 2022, pp. 82-85.
[39] H. Naderiallaf, P. Seri, and G. C. Montanari, "Effect of voltage slew rate on partial discharge phenomenology during voltage transient in HVDC insulation: the case of polymeric cables," IEEE Trans. Dielectr. Electr. Insul., vol. 29, no. 1, pp. 215-222, Feb. 2022.
[40] A. Rumi, J. G. Marinelli, and A. Cavallini, "Converter stress impact on thermally aged resin for low-voltage machines," Annu. Rep. Conf. Electr. Insul. Dielect. Phenom. (CEIDP), 2021, pp. 40-43.
[41] L. Lusuardi, A. Cavallini, M. G. de la Calle, J. M. Martínez-Tarifa and G. Robles, "Insulation design of low voltage electrical motors fed by PWM inverters," IEEE Electr. Insul. Mag., vol. 35, no. 3, pp. 7-15, May-June 2019.
[42] D. R. Meyer, A. Cavallini, L. Lusuardi, D. Barater, G. Pietrini, and A. Soldati, "Influence of impulse voltage repetition frequency on RPDIV in partial vacuum," IEEE Trans. Dielec. Elec. Insul., vol. 25, no. 3, pp. 873-882, 2018.
[43] M. Cacciari, A. Contin, G. C. Montanari, "Use of a mixed-Weibull distribution for the identification of partial discharge phenomena", IEEE Trans. Dielec. Elec. Insul., Vol. 2, n. 6, pp.1166-1179, December 1995.
[44] A. Contin, E. Gulski, M. Cacciari, G.C. Montanari, "Inference of PD in electrical insulation by charge-height probability distribution. Diagnosis of insulation system degradation", IEEE Trans. Dielec. Elec. Insul., Vol. 5, n. 1, pp. 110-117, February 1998.

Hadi Naderiallaf was born in Mashhad, Iran, on April 16, 1986. He received his PhD degree in 2021 from the University of Bologna, Italy, and his M.Sc. degree in 2012 from the Leibniz University Hannover, Germany, both in electrical engineering (high voltage engineering). In 2019, he was a visiting scholar and PhD researcher at the Department of High Voltage Engineering in the Technical University of Berlin, Germany, for three months. Since April 2021, he has been a Postdoctoral Research Fellow at the University of Nottingham, UK. He is currently working on the electrical machine insulation design and reliability aspects for industrial projects, including aerospace (e.g., Clean Sky) and automotive applications. His main research interests are electrical insulating materials, AC and DC partial discharge detection and modelling, insulation systems reliability for electrical machines, HVDC cables design, multiphysics modelling, space charge measurement and analysis, condition monitoring techniques, DGA and transformer oil reclamation.

Paolo Giangrande (M'12-SM'19) received the PhD degree in electrical engineering from the Politecnico of Bari in 2011. He was appointed as Research Fellow and as Senior Research Fellow with the Power Electronics, Machines and Control Group at the University of Nottingham (UK) in 2012 and 2018 respectively. Since 2022, he is Associate Professor in electrical machines and drives at the University of Bergamo (Italy) within the Department of Engineering and Applied Sciences. His main research interests include sensorless control of AC electric drives, design and testing of electromechanical actuators for aerospace, thermal management of high-performance electric drives and lifetime modelling of electrical machines.

Michael Galea received the Ph.D. degree in electrical machines design in 2013 from the University of Nottingham, Nottingham, U.K. He was promoted to Full Professor of Electrical Machines and Drives with the University of Nottingham in 2019. Since 2021, Prof Galea is with the Department of Industrial Electrical Power Conversion of the University of Malta. His main research interests include design and development of electrical machines and drives (classical and unconventional), reliability and lifetime degradation of electrical machines and the more electric aircraft. Michael is a Fellow of the Royal Aeronautical Society and a Senior Member of the IEEE. Michael also serves an Associate Editor for the IEEE Transactions on Industrial Electronics and for the IET Electrical Systems in Transportation.